

See discussions, stats, and author profiles for this publication at: <https://www.researchgate.net/publication/281621266>

# Regulatable and Modulable Background Expression Control in Prokaryotic Synthetic Circuits by Auxiliary Repressor Binding Sites

ARTICLE *in* ACS SYNTHETIC BIOLOGY · SEPTEMBER 2015

Impact Factor: 4.98 · DOI: 10.1021/acssynbio.5b00111

---

READS

15

2 AUTHORS, INCLUDING:



**Davide Merulla**

University of Lausanne

10 PUBLICATIONS 59 CITATIONS

SEE PROFILE

# Regulatable and Modulable Background Expression Control in Prokaryotic Synthetic Circuits by Auxiliary Repressor Binding Sites

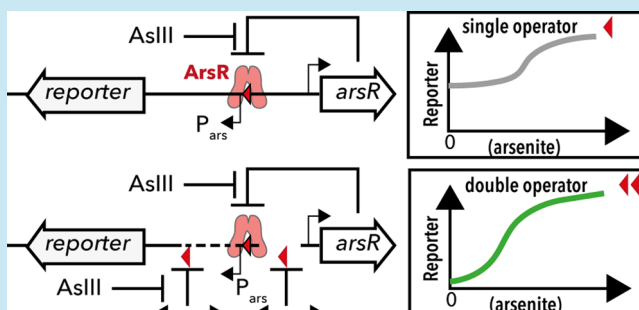
Davide Merulla and Jan Roelof van der Meer\*

Department of Fundamental Microbiology, University of Lausanne, 1015 Lausanne, Switzerland

**S** Supporting Information

**ABSTRACT:** Expression control in synthetic genetic circuitry, for example, for construction of sensitive biosensors, is hampered by the lack of DNA parts that maintain ultralow background yet achieve high output upon signal integration by the cells. Here, we demonstrate how placement of auxiliary transcription factor binding sites within a regulatable promoter context can yield an important gain in signal-to-noise output ratios from prokaryotic biosensor circuits. As a proof of principle, we use the arsenite-responsive ArsR repressor protein from *Escherichia coli* and its cognate operator. Additional ArsR operators placed downstream of its target promoter can act as a transcription roadblock in a distance-dependent manner and reduce background expression of downstream-placed reporter genes. We show that the transcription roadblock functions both in cognate and heterologous promoter contexts. Secondary ArsR operators placed upstream of their promoter can also improve signal-to-noise output while maintaining effector dependency. Importantly, background control can be released through the addition of micromolar concentrations of arsenite. The ArsR-operator system thus provides a flexible system for additional gene expression control, which, given the extreme sensitivity to micrograms per liter effector concentrations, could be applicable in more general contexts.

**KEYWORDS:** bacterial bioreporters, synthetic biology, ArsR, arsenic, repressor protein, operator



A central tenet of synthetic biology is that understanding biological systems can be improved through their reconstruction from individual parts.<sup>1,2</sup> There is, therefore, much current interest in characterizing DNA parts (e.g., genes, promoters) and learning the basic rules to design operational circuits from such parts.<sup>3–8</sup> Gene circuits often consist of an ordered set of operators capable of processing a specific input into a desired biological output.<sup>6,8–13</sup> Current designs rely heavily on parts that allow control at the transcriptional level, such as genes for regulatory proteins that interact with specific DNA binding motifs near promoters. Further system fine-tuning is achieved by using promoters with different strengths<sup>3,7,14</sup> or by controlling it at the post-transcriptional level through the choice of the Shine–Dalgarno sequence (i.e., ribosome binding site or RBS),<sup>4,15</sup> the length and sequence of the 5′-untranslated region (UTR) of the mRNA,<sup>16,17</sup> gene codon usage, or addition of tags for increased rates of protein degradation.<sup>10,17</sup> Despite the wide variety of parts available for expression control and fine-tuning, the operation of gene circuits is frequently hampered by background noise, which occurs as a result of leaky promoters and inherently relaxed control by transcription factors. This is particularly cumbersome for biosensing applications in synthetic biology, which need to be able to accurately quantify the presence of specific target chemicals at low (micrograms per liter) concentrations.<sup>18</sup>

There are remarkably few possibilities to reduce background expression in a circuit while at the same time providing high output and tight control. Transcription terminators are not suitable because they cannot be derepressed in response to an incoming signal. Promoter modifications to increase its strength will result in higher output but, simultaneously, higher background, and vice versa for lower strength promoters. Modifications of transcription factors and their binding sites within promoters can change the equilibrium of the signal's integration but typically do not change the amplitude of the promoter's output.<sup>7,19</sup>

We show here that positioning a secondary regulatory protein binding site (operator) within a given promoter context can yield flexible and modulable fine-tuned transcription control. It is well-known that prokaryotic regulatory proteins can enhance otherwise poorly transcribed promoters in the presence of chemical effectors (activation)<sup>20</sup> or through post-translational modification (e.g., phosphorylation).<sup>21</sup> Alternatively, they can decrease transcription from promoters by effector binding (corepression) or block transcription altogether but can successively release repression through inducer binding (e.g., the well-known LacI–allolactose system of *Escherichia coli*).<sup>22</sup> Regulatory proteins exert control by binding

**Received:** June 17, 2015



73 to precise sequence motifs within or near promoter regions,  
74 and interaction with effectors changes the affinity of regulatory  
75 proteins for their operator and/or alters their interactions with  
76 RNA polymerase.<sup>20,21,23</sup> Since regulatory proteins act by  
77 binding to specific operators, placement of additional copies  
78 of such sequences could alter interactions with RNA polymerase  
79 or sterically obstruct RNA polymerase to continue the  
80 transcription bubble, which could potentially result in improved  
81 background control of downstream-placed genes.

82 In order to demonstrate the general use of auxiliary operator  
83 sites for improved expression control in a synthetic gene circuit,  
84 we systematically tested the effect of placement, orientation,  
85 and sequence of an operator within its cognate and a  
86 heterologous promoter context. As a proof of concept and,  
87 additionally, to show the usefulness of designing a modifiable  
88 background controlled synthetic circuit, we focus on the ArsR  
89 system of *E. coli*. Arsenic biosensors have to give accurate  
90 responses well below 10  $\mu\text{g}$  of  $\text{As L}^{-1}$  in order to measure  
91 environmentally and medically relevant concentrations.<sup>24</sup> We  
92 employed the well-characterized ArsR repressor from *E. coli*  
93 plasmid R773, which confers enhanced resistance to arsenic.<sup>25</sup>  
94 ArsR controls transcription from the  $P_{\text{ars}}$  promoter by binding  
95 as a homodimer to an operator site directly upstream of  $P_{\text{ars}}$   
96 (Supporting Information Figure S1).<sup>26</sup> ArsR repression is  
97 released in the presence of arsenite oxyanions that bind to ArsR  
98 with a stoichiometry of two arsenite per dimer, causing a  
99 conformational change in the protein that reduces affinity for  
100 the operator.<sup>27</sup> First, we systematically varied the placement of  
101 a secondary ArsR operator up- or downstream of its original  
102 promoter  $P_{\text{ars}}$  and studied arsenite-dependent reporter output  
103 in a biosensing gene circuit in *E. coli* (Figure 1A). In order to  
104 demonstrate that the system can work in a heterologous  
105 promoter environment, we positioned the ArsR operator within  
106 the 2-hydroxybiphenyl (2HBP)-inducible  $P_{\text{C}}$  promoter of  
107 *Pseudomonas azelaica*, which is controlled by the XylR-type  
108 transcription activator, HbpR.<sup>28</sup> Northern hybridizations were  
109 used to demonstrate that downstream placement of a  
110 secondary ArsR operator yields a transcription roadblock.  
111 Our results show how auxiliary operator placement can provide  
112 a general tool to fine-tune background expression levels in gene  
113 circuitry and illustrate how this can help to engineer biosensors  
114 with environmentally and medically relevant detection capacity.

## 115 ■ RESULTS AND DISCUSSION

### 116 A Secondary Downstream ArsR Binding Site Reduces 117 Background Expression But Retains Induction from $P_{\text{ars}}$ .

118 In order to determine whether secondary operator sites could  
119 reduce background expression from a reporter gene, we created  
120 a series of  $\text{arsR-}P_{\text{ars}}$  gene circuits in *E. coli* with either a single  
121 ArsR operator within  $P_{\text{ars}}$  or an additional one further  
122 downstream from  $P_{\text{ars}}$  but upstream of an *egfp* reporter gene  
123 (Figure 1A). For proper comparison between constructs with a  
124 single or double ArsR operator(s), we maintained, as closely as  
125 possible, the length and DNA sequence of the 5'-untranslated  
126 region (UTR) of the *egfp* mRNA (Figure 1B,C). The longest  
127 5'-UTR was based on the original sequence downstream of  $P_{\text{ars}}$   
128 in plasmid R773 (GenBank accession no. X16045.1; Support-  
129 ing Information Figure S2). In the construct with a single ArsR  
130 operator and the longest 5'-UTR of *egfp* (plasmid pAA-1ABS  
131 +425, Figure 1C), EGFP is induced only 2-fold at 100  $\mu\text{g}$  of As  
132  $\text{L}^{-1}$ , as a result of high background expression in the absence of  
133 arsenite (Figure 1D). Successive shortening of the distance  
134 between the  $P_{\text{ars}}$  promoter and *egfp* slightly improves the

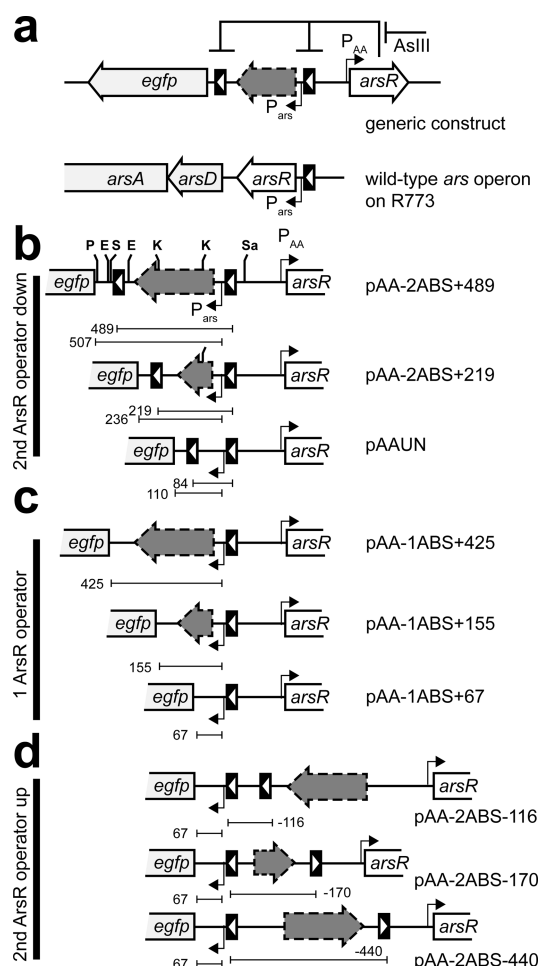


**Figure 1.** Schematic representation of the different gene circuits used in this work. (A) Generic outline of the *arsR*-dependent reporter circuit and the native configuration of the *arsR* operon. In the generic construct, *arsR* is expressed from the constitutive  $P_{\text{AA}}$  promoter and represses transcription from the  $P_{\text{ars}}$  promoter, thus repressing *egfp*. In the presence of arsenite ( $\text{AsIII}$ ), repression is relieved and reporter gene expression is enhanced. In the native *ars* operon configuration, ArsR controls its own expression and that of the downstream located genes (*arsDABC*) in an arsenite-dependent manner. (B) Details of the circuits with a second ArsR operator (black box with a white triangle) downstream of that in  $P_{\text{ars}}$ . (C) Same as in (B) but for constructs with only one operator. (D) Same as in (B) but for constructs having a second operator upstream of  $P_{\text{ars}}$ . Thin lines indicate lengths of the corresponding *egfp* 5'-UTR and the relative distance between the operators. Gray dotted arrows indicate length and orientation of the intervening DNA (for sequence details, see Supporting Information Figure S2). Restriction sites: E, *EcoRI*; K, *KpnI*; P, *PsiI*; Sa, *SacI*; S, *SpeI*.

induction potential of the system, but the background expression remains high (Figure 2B,D).

In contrast, constructs with similar lengths and sequences of 5' *egfp* UTRs but with an additional ArsR operator downstream of  $P_{\text{ars}}$  and directly upstream of *egfp* displayed a comparatively much lower background signal (Figure 2A). EGFP fluorescence in the double ArsR operator circuits at the same arsenite concentration diminishes with increasing length of the spacer region (Figure 2A). Importantly, however, the fold induction of the signal remains much higher compared to that of constructs having only one operator (Figure 2C). Shortening the distance between the two operator copies improves both absolute EGFP

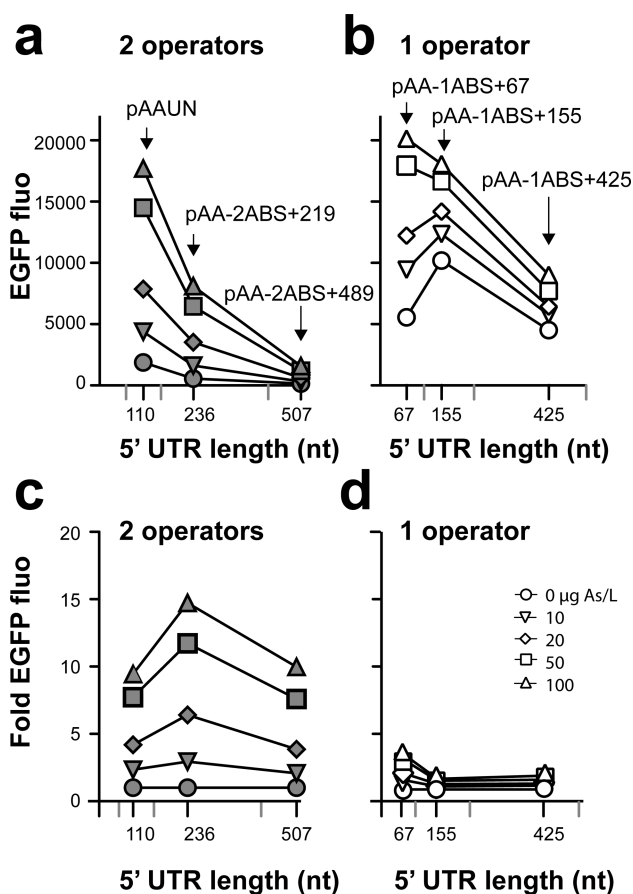


**Figure 2.** Effect of 5'-UTR spacer length and downstream distance of the secondary ArsR operator on arsenite-inducible EGFP fluorescence. (A) EGFP fluorescence in cells with a secondary ArsR operator downstream, induced or uninduced for 2 h with arsenite at different concentrations. (B) Same as in (A) for single-operator constructs. Relevant plasmid names are indicated. Data points are averages from mean cell fluorescence by flow cytometry from triplicate biological incubations. Error bars (as standard deviation from the average) are smaller than the data symbols. (C, D) Data from (A) and (B), respectively, but expressed as the ratio between the average EGFP fluorescence in the arsenite-containing sample and that of cells in buffer without arsenite (fold EGFP). nt, nucleotide. UTR, untranslated spacer region.

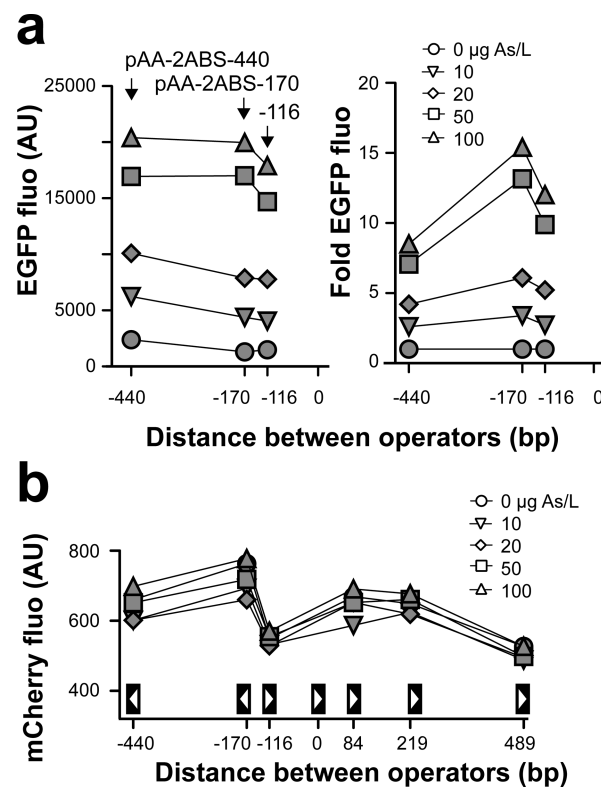


**Figure 3.** Effect of positioning the second ArsR operator upstream within the *arsR-egfp* circuitry. (A) EGFP fluorescence and fold change as a function of distance between the two ArsR operators after a 2 h induction with different arsenite concentrations, as measured by flow cytometry. Data points are averages from mean cell fluorescence by flow cytometry in triplicate biological incubations. Error bars (as standard deviation from the triplicate average) are smaller than the data symbols. (B) Control constructions with *arsR-mCherry* instead of *arsR* showing ArsR-mCherry fluorescence as a function of distance between the ArsR operators at different arsenite concentrations. For EGFP measurements of these constructs, see Supporting Information Figures S3. White triangles represent the direction of the second operator relative to the operator within the  $P_{ars}$  promoter.

remained very high (Figure 3A). When considering the fold 166 induction, the upstream-placed secondary operators were, 167 therefore, as effective as the downstream placed variants 168 (Figure 3A). Optimal signal-to-noise ratios (up to 15-fold 169 induction at  $50 \mu\text{g}$  of  $\text{As L}^{-1}$ ) occurred at relative distances of 170 170–219 bp up- or downstream, diminishing to 6-fold at 171 shorter and longer relative distances (Figures 2C and 3A). 172 Since the absolute EGFP fluorescence signal is more than 2- 173 fold higher at the same arsenite concentration from plasmid 174 pAA-2ABS-170 than that from pAA-2ABS+219, placing a 175 second operator upstream is actually more favorable for signal 176 detection (Figure 4A,B). On the other hand, the variants with 177 the second ArsR operator downstream show a more efficient 178 reduction of the background signal in the absence of arsenite 179 (Figure 4A). 180

Because effects of operator placement on *egfp* expression 181 may be masked by varying ArsR levels in the different 182 constructs, we examined the expression of ArsR from  $P_{AA}$ . 183 Here, we used similar plasmid constructs as those in Figure 1 184 but replaced *arsR* with an *arsR-mCherry* translational fusion. 185 Constructs producing ArsR-mCherry instead of ArsR showed 186 slightly lower EGFP fluorescence levels, and the fold inductions 187 were less pronounced (Supporting Information Figure S3). 188

147 signal intensity and fold induction: from 10-fold at 489 bp 148 distance to 15-fold at 219 bp and at  $100 \mu\text{g}$  of  $\text{As L}^{-1}$  (Figure 149 2C). At shorter ArsR operator distances (e.g., in pAA-2ABS 150 +67), the absolute EGFP intensity increases further, but the 151 induction level decreases (Figure 2C). Reduction of back- 152 ground EGFP expression is thus not an effect of the 5'-UTR 153 sequence or its length, but it is due to the second operator and 154 its interactions with ArsR.

155 **Decreased Background Expression from Upstream-**  
156 **Placed ArsR Binding Sites.** Next, we systematically tested the 157 effect of placement of a secondary ArsR operator, now placed 158 upstream of the *ars* promoter, in a series of reporter circuits 159 with operator–operator distances of 116, 170, and 440 bp 160 (Figure 1D). Surprisingly, an upstream-placed secondary ArsR 161 operator also reduced background EGFP reporter expression in 162 the absence of arsenite, almost to the level of placing the 163 second ArsR operator immediately downstream of the 164 transcriptional start site (Figure 3A). On the contrary, the 165 EGFP fluorescence levels in cells upon addition of arsenite



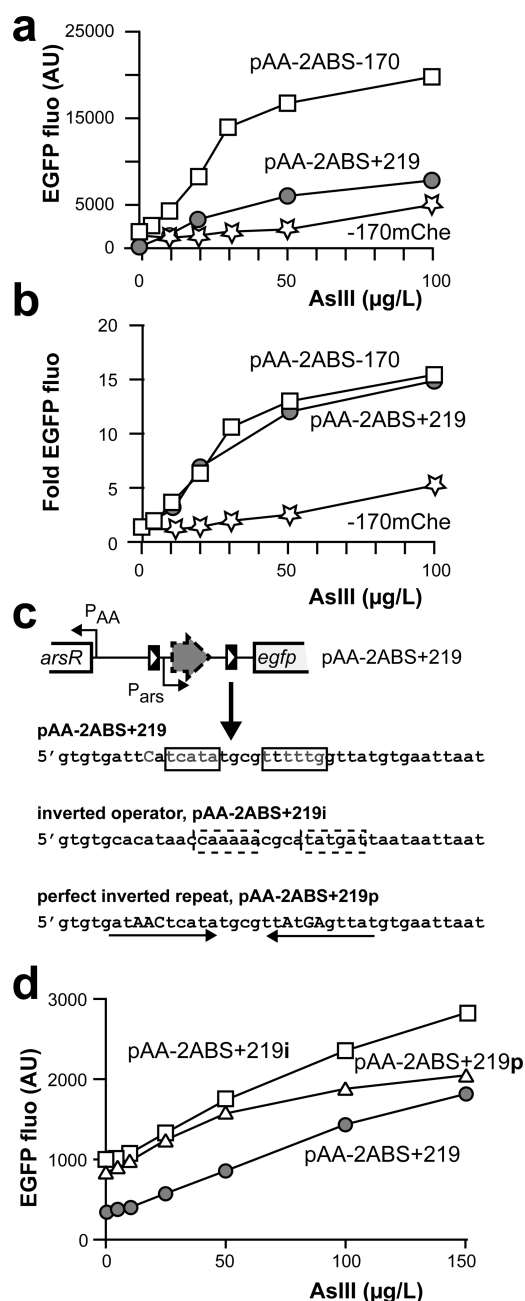


**Figure 4.** Performance of the *E. coli* arsenite bioreporters. (A) Average EGFP fluorescence from two optimized double ArsR operator constructs as a function of arsenite concentration after a 2 h induction. (B) Same as in (A) but displaying fold induction. (C) ArsR operator orientation and sequence. Boxes point to experimentally determined ArsR contacts on the DNA.<sup>26</sup> (D) Average EGFP fluorescence in *E. coli* with plasmid pAA-ABS+219p (perfect palindrome), pAA-ABS+219i (inverted operator), or pAA-ABS+219 as a function of arsenite concentration (from 0 to 150 μg L<sup>-1</sup>) after 190 min of exposure measured by flow cytometry (error bars are smaller than the data symbols).

that effects of dual operator placement within the global 196 environment of the P<sub>ars</sub> promoter are due to ArsR interacting 197 with the operator, not to fluctuating levels of ArsR itself. 198

**Heterologous Application of the ArsR Operator as a Transcriptional Roadblock.** To test whether the ArsR- 200 operator system can be used to reduce background expression 201 in a heterologous promoter context (i.e., non-arsR origin), we 202 constructed circuits in which *egfp* reporter gene expression is 203 controlled by the HbpR activator protein.<sup>28,29</sup> HbpR is a σ<sup>54</sup>- 204 RNA polymerase-dependent transcription factor from *Pseudo-* 205 *monas azelaica*, which activates the P<sub>C</sub> promoter upstream of 206 the *hbpC* gene in the presence of the effector 2- 207 hydroxybiphenyl (2HBP).<sup>29</sup> EGFP fluorescence is about 35- 208 fold induced after a 2 h incubation with 10 μM 2HBP in *E. coli* 209 carrying plasmids pHBP269 (without ArsR operator) and 210 pGEM-pAA-arsR, a plasmid in which ArsR is constitutively 211 expressed from the P<sub>AA</sub> promoter (Figure 5A). EGFP 212 expression from the P<sub>C</sub> promoter on pHBP269 is not 213 influenced by the presence of subtoxic amounts of arsenite 214 between 5 and 100 μg L<sup>-1</sup>. Inclusion of the ArsR operator 215 downstream of the P<sub>C</sub> promoter but upstream of *egfp*, as in 216 pHBP-ABS-dir1, makes the reporter circuit dependent on ArsR 217 and reduces EGFP expression 4-fold in the absence of arsenite 218 (Figure 5B,D). Addition of arsenite to *E. coli* carrying pHBP- 219 ABS-dir1 and pGEM-pAA-arsR relieves ArsR control in an 220 arsenite-concentration-dependent manner, with absolute EGFP 221 expression levels after 2HBP induction being restored to 70% at 222 100 μg of AsIII L<sup>-1</sup> and fold-induction being almost completely 223 restored to the level in the P<sub>C</sub> promoter context without an 224 ArsR operator (Figure 5B). 225

To confirm that the control exerted by the added 226 heterologous ArsR operator occurs at the transcriptional level, 227 we compared, by northern hybridization, P<sub>C</sub>-driven mRNA 228 expression from pHBP plasmids with or without the ArsR 229 operator (Figure 6A). RNA was hereto isolated from cultures 230 fully induced by 10 μM 2HBP in the presence or absence of 231 100 μg L<sup>-1</sup> arsenite. Hybridizing size-separated and blotted 232 RNAs with a probe targeting *egfp* mRNA showed that 233 transcription from the P<sub>C</sub> promoter on pHBP269 is much 234 stronger than that from pHBP-ABS-dir1 (Figure 6C), whereas 235 transcription of the plasmid-located Km gene is similar (Figure 236 6B). Addition of arsenite to the cells does not influence the 237 amount of *egfp* mRNA from P<sub>C</sub> with plasmid pHBP269, but it 238 increases it with plasmid pHBP-ABS-dir1, as expected when 239 repression by ArsR is released through arsenite (Figure 6C). 240 Derepression by arsenite in pHBP-ABS-dir1 was not complete, 241 as *egfp* mRNA did not reach the same levels in cells with 242 pHBP-ABS-dir1 as it did in cells with pHBP269. When 243 targeting the same transcript with a specific probe directly 244 downstream of the transcription start site, we observed strongly 245 diminished transcription in the case of pHBP-ABS-dir1 246 compared to that of pHBP269 and partial restoration after 247 addition of arsenite (Figure 6D). We did not observe a very 248 small (110 nucleotides) specific mRNA in cells carrying 249 plasmid pHBP-ABS-dir1, which might be formed when RNA 250 polymerase aborts transcription at the ArsR operator. Although 251 hybridization showed a small RNA, this signal was present in all 252 lanes including RNA from *E. coli* devoid of any plasmid and is 253 thus probably due to nonspecific binding (Figure 6D). 254

**Background Reduction Is Dependent on the Sequence and Orientation of the ArsR Operator.** In order 255 to test the effect of the ArsR operator's orientation on 256 background reduction, we inverted the operator in plasmid 257

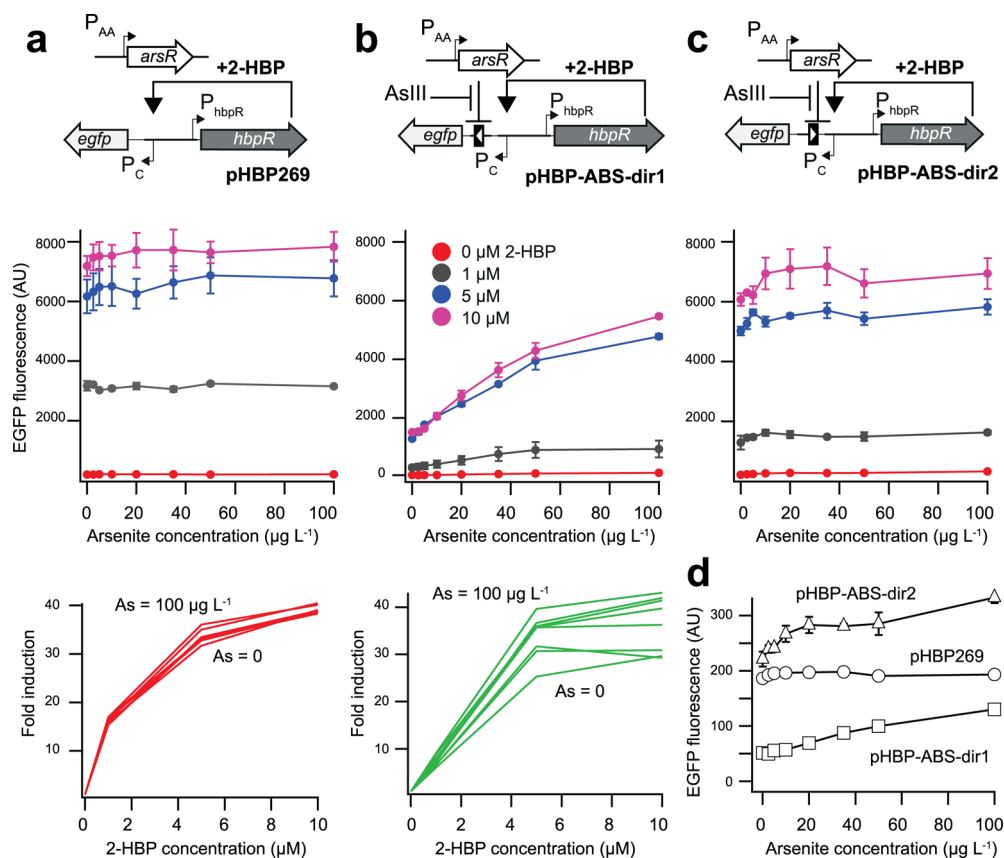


**Figure 5.** Effect of the ArsR-operator on expression from the heterologous HbpR-P<sub>C</sub> system. (A) Triplicate-averaged absolute EGFP fluorescence (via flow cytometry) or fold-induction in *E. coli* cells that express *egfp* from P<sub>C</sub> on plasmid pHPB269 and are cotransformed with pGem-pAA-arsR as a function of arsenite concentration (from 0 to 100 μg L<sup>-1</sup>) and 2-hydroxybiphenyl (2-HBP) addition (from 0 to 10 μM). (B) Same as in (A) but in *E. coli* carrying pHPB-ABS-dir1 plus pGem-pAA-arsR. (C) Same as in (B) but with the opposite orientation of the ArsR operator within the P<sub>C</sub> promoter (pHPB-ABS-dir2) plus pGem-pAA-arsR. The white triangle notes the position and orientation of the ArsR-operator. For sequence details, see Supporting Information Figure S6. (D) Background reduction as a function of ArsR operator orientation and arsenite concentration without addition of 2-HBP.

259 pAA-2ABS+219 and evaluated its inducibility with arsenite  
260 (Figure 4C,D). Although its inducibility with arsenite remained,  
261 the background EGFP expression was 3-fold lower in pAA-  
262 2ABS+219 than it was in pAA-2ABS+219i with the inverted  
263 ArsR operator (Figure 4C). Inverting the ArsR operator within  
264 the P<sub>C</sub> promoter context (as in pHPB-ABS-dir2) also alleviated  
265 the background control, and only very slight repression by ArsR  
266 remained (Figure 5C,D). This showed that downstream ArsR  
267 operator control is orientation-dependent. Finally, we replaced  
268 the (imperfect) palindromic sequence within the native  
269 operator with a perfect palindrome, pAA-2ABS+219p (Figure  
270 4C). Interestingly, this changed the response to increasing  
271 arsenite concentration, but it did not result in a lower  
272 background expression in the absence of arsenite compared  
273 to that with pAA-2BA+219 (Figure 4D).

274 **Secondary Operators Downstream Reduce Back-**  
275 **ground Expression by Acting as a Transcription Road-**  
276 **block.** This raises the question as to what the actual  
277 mechanism(s) for the observed diminished background gene  
278 expression upon placement of a secondary ArsR operator  
279 downstream of the promoter is. Most likely, the ArsR protein  
280 maintains the same mechanism of interaction with its operator  
281 and with the effector, causing it to have a higher tendency to  
282 bind the operator in the absence of the effector and a lower  
283 tendency in the presence of the effector.<sup>26</sup> ArsR binding to the  
284 operator DNA far downstream of a promoter may thus lead to

a physical obstruction for RNA polymerase (a true roadblock)  
and lead to the abortion of transcription at that position.<sup>23,30</sup>  
Our data on the heterologous HbpR-P<sub>C</sub>-ArsR operator system  
indicates that the effect takes place at the transcriptional level  
(Figure 6C) because the levels of *egfp* mRNA from P<sub>C</sub> are  
much lower with an upstream heterologous ArsR operator than  
they are without it and because arsenite addition increases *egfp*  
mRNA levels (Figure 6C). Although we had expected that, in  
that case, a very small mRNA fragment comprising the region  
between the transcriptional start and the roadblock would arise,  
we were unable to detect this. The reason for this may be that  
the short fragment is rapidly degraded and cannot accumulate  
sufficiently to be detectable by hybridization.

An additional piece of circumstantial evidence for the  
roadblock hypothesis is that transcription repression shows  
directionality (Figures 4D and 5D). Only in the case of its  
native orientation with respect to the promoter (e.g., as in  
plasmid pHPB-ABS-dir1 or pAA-2ABS+219) does the ArsR  
operator function to reduce background expression in the  
presence of ArsR, whereas in the opposite direction (i.e., in  
plasmids pHPB-ABS-dir2 and pAA-2ABS+219i), the effect was  
practically lost (Figures 4D and 5D). This suggests that the  
manner or orientation in which the ArsR repressor dimer binds  
to the operator determines its ability to inhibit RNA  
polymerase. One could imagine that the imperfect dyad  
symmetry of the operator (Figure 4C, Supporting Information 310

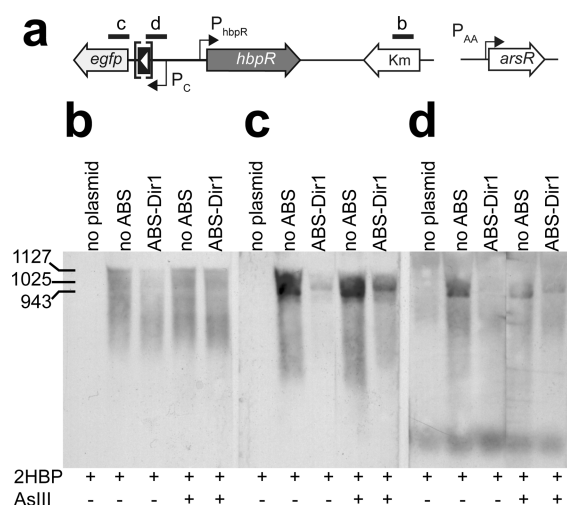


**Figure 6.** Effect of the ArsR-operator on transcription from  $P_C$  in presence or absence of arsenite, as measured by northern analysis. (A) Outline of the *arsR*- and *hbpR*-dependent gene circuits with the location of the hybridization probes used indicated (b, c, and d). (B) Expression of the *Km*-resistance gene on plasmid pHBP269 (no ArsR operator) or pHBP-ABS-dir1 in exponentially growing *E. coli* cotransformed with pGem-pAA-arsR, induced for 30 min with 10  $\mu$ M 2HBP alone or with 10  $\mu$ M 2HBP and 100  $\mu$ g  $L^{-1}$  AsIII. (C) Hybridization with a probe for the *egfp* transcript. (D) Hybridization with a probe specific for the 5'-UTR region of the *egfp* transcript.

sites were not considered in this study.<sup>23</sup> We thus expect that upon placement of the second ArsR operator between  $P_{arsR}$  and *egfp* (Figure 1B) transcription of the reporter gene will occur only when, incidentally, ArsR liberates both the first and second operators or when RNA polymerase occludes or dislodges ArsR from the second operator. The background expression reduction in this case is thus a result of the diminished likelihood that both ArsR operators are free; the probability of this happening is the product of the individual probabilities that each of the ArsR operators is unoccupied. In the case of arsenite being present, the change in ArsR-As<sub>III</sub>-operator binding affinity<sup>26</sup> largely increases the likelihood of both operators being simultaneously liberated, and the reporter gene *egfp* is again expressed at a high rate. One would thus have expected that at high arsenite concentrations of, e.g., 100  $\mu$ g  $L^{-1}$ , ArsR repression would have been completely relieved and that EGFP expression would be the same for both systems with one or two ArsR operators, but this was observed only for the shorter 5'-UTR distance (Figure 2A,B). Perhaps this is a result of slight sequence differences between the 5'-UTR spacers, which were due to placement of the second ArsR operator (Figure 1B,C).

**Increased Local Repressor Concentration at Dual Upstream Operators.** Unexpectedly, we discovered that the second ArsR operator copy can also improve gene expression control when it is placed further upstream of the promoter, at least in the case of  $P_{ars}$  (Figure 3). It is unlikely that in this case the ArsR dimer functions as a transcription roadblock; rather, the effect might be due to an increased concentration of repressor in the vicinity of the promoter. Hammar et al.<sup>22</sup> recently proposed that the LacI repressor finds its operator site by scanning with low specificity along the DNA, sliding several times back and forth within a  $45 \pm 10$  bp region. This scanning behavior would increase the probability of LacI binding to the operator from 7 to  $53 \pm 24\%$  of the times it contacts the area.<sup>22</sup> A direct consequence of this behavior is that the concentration of repressor in the proximity of an operator sequence would be higher than it is elsewhere. If we assume that this model applies for ArsR, too, then two closely spaced operators will synergistically increase repressor concentration and ultimately lead to better repression (Supporting Information Figure S5), and this effect should be independent of the relative orientation of the operators. In contrast, the efficiency would be dependent on the inter-operator distance: at distances too far for the sliding windows to overlap, the effect will be negligible, whereas at close proximity, collisions between sliding repressors may occur, leading to steric hindrance and repression inhibition. This hypothesis could explain the arsenite-dependent EGFP induction observed when placing the second ArsR operator at different distances upstream of  $P_{ars}$  (e.g., Figure 4). The slightly different results obtained with the ArsR-mCherry variants do suggest that steric hindrance can reduce the effect of locally increased repressor concentrations (Supporting Information Figure S3B,C).

## CONCLUSIONS

In contrast to transcription terminators, the deployment of regulatory proteins and their DNA binding sites could be a means to reduce background expression in genetic circuits but maintain inducible control. As a proof of principle, we used the ArsR repressor and its native operator.<sup>26</sup> Our results clearly show that adding a second copy of the operator for ArsR diminishes reporter gene expression in the absence of effector

Figure S1) causes the two ArsR DNA binding domains in the dimer to bind to the operator with different affinities. Changing the orientation of the ArsR operator might bring the repressor dimer to face the approaching RNA polymerase with either the strongly or weakly bound side (Supporting Information Figure S4). In the proper orientation, the ArsR dimer could work as a molecular wedge, stopping the approaching RNA polymerase, whereas in the other orientation, it could be peeled off more easily by RNA polymerase, resulting in less effective transcription abortion (Supporting Information Figure S4). Attempts to improve the background reduction effect by creating a perfect palindromic ArsR operator were unsuccessful (i.e., plasmid pAA-2BAS+219p; Figure 4C,D), suggesting that it is the binding affinity and orientation that are important for it to work as roadblock. An alternative scenario is that in the proper orientation the ArsR repressor dimer is contacting the strand that is being transcribed, whereas in the other orientation, it binds on the opposite strand and does not inhibit RNA polymerase (Supporting Information Figure S4). This may be worthwhile to unravel in future work in order to possibly further improve the use and effect of operators in a heterologous or orthogonal promoter context.

Recent experimental and modeling work on transcriptional readthrough using single-copy LacI operators suggests that the magnitude of a transcriptional roadblock is dependent on the strength of the promoter, the unbinding constant of LacI to its operator, and the concentration of LacI.<sup>23</sup> These LacI-*lacO* models further suggest that single RNA polymerases at low promoter firing rates can actively dislodge LacI at its *lacO* position but that at high promoter firing rates, multiple individual RNA polymerases transcribing the 5'-leader region may become clogged upstream of the bound LacI to *lacO* or may occlude the binding site from access to LacI. However, a clear distance effect of *lacO* positioning to the promoter on the road-blocking magnitude was not detected, and double *lacO*



Table 1. Relevant Bacterial Strains Used in This Work

strain no.	relevant genotype	plasmid	description	ref
3304	<i>Escherichia coli</i> MG1655 $\Delta$ arsRBC		chromosomal deletion of <i>arsRBC</i>	29
3391	based on 3304	pAAUN = (pAA-2ABS+84)	second ABS <sup>1</sup> 84 bp downstream, 110 nt 5'-UTR of <i>egfp</i>	29
4144	based on 3304	pAA-2ABS+219	second ABS at 219 bp downstream, 236 nt 5'-UTR of <i>egfp</i>	this study
4093	based on 3304	pAA-2ABS+489	second ABS 489 bp downstream, 507 nt 5'-UTR of <i>egfp</i>	this study
4351	based on 3304	pAA-2ABS-116	second ABS 116 bp upstream	this study
4356	based on 3304	pAA-2ABS-170	second ABS 170 bp upstream	this study
4352	based on 3304	pAA-2ABS-440	second ABS 440 bp upstream	this study
4223	based on 3304	pAA-1ABS+67	single ABS, 67 nt 5'-UTR of <i>egfp</i>	this study
4484	based on 3304	pAA-1ABS+155	single ABS, 155 nt 5'-UTR of <i>egfp</i>	this study
4380	based on 3304	pAA-1ABS+425	single ABS, 425 nt 5'-UTR of <i>egfp</i>	this study
3667	based on 3304	pAAUN-mChe = pAA-2ABS+84-mChe	second ABS at 84 bp downstream, 110 nt 5'-UTR of <i>egfp</i> , <i>arsR-mCherry</i> fusion	29
4360	based on 3304	pAA-2ABS+219-mChe	second ABS at 219 bp downstream, 236 nt 5'-UTR of <i>egfp</i> , <i>arsR-mCherry</i> fusion	this study
4233	based on 3304	pAA-2ABS+489-mChe	second ABS at 489 bp downstream, 507 nt 5'-UTR of <i>egfp</i> , <i>arsR-mCherry</i> fusion	this study
4300	based on 3304	pAA-1ABS+67-mChe	single ABS, 67 nt 5'-UTR of <i>egfp</i> , <i>arsR-mCherry</i> fusion	this study
4353	based on 3304	pAA-2ABS-116-mChe	second ABS 116 bp upstream, <i>arsR-mCherry</i> fusion	this study
4355	based on 3304	pAA-2ABS-170-mChe	second ABS 170 bp upstream, <i>arsR-mCherry</i> fusion	this study
4354	based on 3304	pAA-2ABS-440-mChe	second ABS 440 bp upstream, <i>arsR-mCherry</i> fusion	this study
4486	based on 3304	pHBP269/pGem-pAA-ArsR	<i>hbpR</i> , <i>P<sub>C</sub>-egfp</i> fusion, <i>arsR</i> under <i>Plac</i>	37 and this study
4487	based on 3304	pHBP269-dir1/pGem-pAA-ArsR	as 4486, but ABS downstream of <i>P<sub>C</sub></i>	this study
4488	based on 3304	pHBP269-dir2/pGem-pAA-ArsR	as 4486, but ABS downstream of <i>P<sub>C</sub></i> in opposite orientation	this study
4480	based on 3304	pAA-2ABS+219p	as 4144, but second ABS with perfect dyad symmetry	this study
4481	based on 3304	pAA-2ABS+219i	as 4144, but second ABS in opposite orientation	this study

<sup>a</sup>ABS, ArsR binding site (ArsR operator).

(arsenite) but that the repression is released in an arsenite-dependent manner. In effect, therefore, the placement of a second copy of the operator resulted in a largely improved signal-to-noise ratio: from 2- to 3-fold in the system with only the single cognate ArsR operator within *P<sub>ars</sub>* to 10–15-fold in the comparable case of a second operator (Figures 2C,D and 3A). We also showed that the regulatable background reduction effect of the ArsR-operator system is not confined to the cognate *ars* operon environment but that it can function within a completely different heterologous promoter background. For this, we chose the *P<sub>C</sub>* promoter, which originates from a completely different species (*P. azelaica* instead of *E. coli*), is controlled by an activator (HbpR) instead of a repressor (ArsR), and that functions with  $\sigma^{54}$  rather than  $\sigma^{70}$ -RNA polymerase (ArsR-*P<sub>ars</sub>*).<sup>29</sup> Coexpressing ArsR in the same cell as HbpR resulted in a 5-fold decrease in reporter expression and a 4-fold decrease in background expression, which could both be relieved to 70% in an arsenite-concentration-dependent manner (Figure 5D). It is likely that further optimization can be obtained by refining the placement of the ArsR binding site within the context of *P<sub>C</sub>*. The concept of modulable background control on inducible promoters should be generally applicable and is therefore of great interest for synthetic biology applications, taking into consideration both the actual data on the ArsR-operator presented here and inferring behavior from, e.g., the use of (single) LacI operators as a transcription roadblock.<sup>23</sup> We also believe that the ArsR-operator system itself is more widely applicable and can complement existing typical conceptual promoter tools such as LacI/*P<sub>lac</sub>* or TetR/*P<sub>tet</sub>* since arsenite concentrations that are needed to relieve ArsR-operator control are very low (micromolar range).

On a practical level, our results showed that it is possible to further improve *E. coli*-based bioreporters for arsenic detection, which have proven to be very valuable in field testing potable water sources for arsenic contamination in exposed areas.<sup>24,31</sup> The improvement that this study brings to existing bioreporters is that it can further increase the absolute signal output of the cells (e.g., as in variant pAA-2ABS-170) while maintaining a very good signal-to-noise ratio of 15-fold induction at 100  $\mu$ g of As L<sup>-1</sup>. Incidentally, the ArsR-mCherry variants may be useful for more accurate quantification at arsenite concentration between 50 and 100  $\mu$ g L<sup>-1</sup> because of their linearity of response, even though they produce, overall, lower EGFP signals than the ArsR variants (Figure 4A,B). We therefore believe that the findings reported here have both general significance for synthetic biology approaches to provide additional expression control mechanisms and practical significance for improving bioreporter constructs to easily and affordably measure arsenic in contaminated regions.<sup>32,33</sup>

## METHODS

**Strains and Culture Conditions.** All strains, plasmids, and relevant characteristics are listed in Table 1. All strains are based on *E. coli* MG1655  $\Delta$ RBC, a strain in which the chromosomal *arsRBC*-operon is deleted.<sup>34</sup> *E. coli* strains were cultured on LB medium<sup>35</sup> at 37 °C with inclusion of the appropriate antibiotics to maintain the plasmid reporter constructs, except during bioreporter assays (see below).

**ArsR Operator Designs in Homologous *ars* Setting.** The initial design consisted of an uncoupled variant of the natural *P<sub>ars</sub>* *arsR* feedback system, in which *arsR* is placed under control of the constitutive *P<sub>AA</sub>* promoter and is divergently



oriented to the *egfp* gene, which is under control of the  $P_{ars}$  promoter (Figure 1A).<sup>34</sup> Three variants were produced in which an extra copy of the ArsR operator was placed upstream of *egfp* but at increasing distances downstream of the transcription start site (Figure 1B). The sequence used for the spacer region consisted of a frameshift *arsR* gene sequence to be able to compare distance effects between the variants having two ArsR operators versus those having only a single operator. A 576 bp region consisting of the ArsR operator followed by  $P_{ars}$  and *arsR* and then another ArsR operator sequence, as in ref 36, was *de novo* synthesized (DNA2.0, Inc.) but with addition of 5' *SacI* and 3' *PsiI* sites and with an extra C nucleotide at position 30 to introduce a frame shift mutation in *arsR* (Supporting Information Figure S2). This results in stop codons at position 31, 46, 103, and 256. Furthermore, positions 156 and 426 were mutated to create two *KpnI* sites. By replacing the *SacI*–*PsiI* fragment of the previously described plasmid pAAUN<sup>34</sup> with the newly synthesized piece, we produced plasmid pAA-2ABS+489, in which the distance between the two operators is 489 bp (Figure 2). Next, by removing the 270 bp *KpnI*–*KpnI* fragment and self-ligation, we produced pAA-2ABS+219 (distance between the operators of 219 bp). Variants carrying a single operator were then produced from pAAUN, pAA-2ABS+489, and pAA-2ABS+219 by *EcoRI* digestion and recircularization, which removes an 81 bp fragment containing the secondary operator proximal to *egfp* (resulting in plasmids pAA-1ABS+67, pAA-1ABS+425, pAA-1ABS+155, respectively; Figure 1C).

Next, we created a set of plasmids in which the second operator is located at varying distances upstream of the  $P_{ars}$  promoter (Figure 1D). First, by using primers 120903 (GAGCTCTGTTGCAACTAACACCACTTCAG) and 120904 (TCTTTAGTTAGTTAGGGAATTCAGTAGTG) in a polymerase chain reaction (PCR), we amplified the fragment between both ArsR operators of pAA-2ABS+489 while adding a *SacI* restriction site at its 3' end. After gel extraction and purification, the fragment was inserted via TA cloning in pGEM-T-Easy (Promega). The orientation and sequence of the insert were verified. The part containing the secondary ArsR operator was retrieved by digestion with *SacI* and cloned into the *SacI* site of pAA-1ABS+67. Depending on the orientation of the insert, this produced plasmids pAA-2ABS-116 and pAA-2ABS-440 (Figure 1D). Finally, by removing, by *KpnI* digestion, the internal fragment in pAA-2ABS-440, we produced plasmid pAA-2ABS-170 (Figure 1D). All procedures were subsequently repeated starting from plasmid pAAUN-mChe, which carries an *arsR*-mCherry fusion gene<sup>34</sup> and enables measurement of ArsR-mCherry levels in the cells (Figure 3B). All inserts were validated by sequencing.

To test the effect of ArsR operator orientation and sequence on expression, appropriate gene blocks were synthesized (150 bp gBlocks, Integrated DNA Technologies) that could be directly replaced by *SpeI* and *KpnI* restriction digestion in pAA-2ABS+219. After transformation, this resulted in plasmids pAA-2ABS+219p (perfect dyad symmetry, 5'-ATAACTCATATGCGTTATGAGTTATGTG) and pAA-2ABS+219i (inverted ABS, 5'-CACATAACCAAAAACGCATATGATTAAT, Figure 4C). Both constructs were validated by sequencing.

**Design of Reporter Circuits with the ArsR Operator in Heterologous Environment.** To test whether the ArsR operator system could control a heterologous inducible promoter, we used the HbpR/ $P_C$  promoter from *P. azelaica* HBPI.<sup>29</sup> As a starting point and native control, we used *E. coli*

with plasmid pHBP269 (our strain collection no. 1855), which carries both the *hbpR* gene and, divergently oriented, the *egfp* gene under control of the  $P_C$  promoter.<sup>37</sup> The ArsR operator was inserted downstream of the  $P_C$  promoter on pHBP269 by recovering an 81 bp *EcoRI*–*EcoRI* fragment from pPR-arsR-ABS<sup>36</sup> and inserting this in both orientations into the unique *EcoRI* site on pHBP269 (Figure 5A, Supporting Information Figure S6). After transformation into *E. coli*, this resulted in plasmids pHBP-ABS-dir1, in which the operator is in the native orientation with respect to the direction of the  $P_C$  (and  $P_{ars}$ ) promoter, and pHBP-ABS-dir2, in which the operator is in the opposite direction (Figure 5B,C). To exert ArsR control, the *E. coli* strains were additionally transformed with plasmid pGEM-pAA-ArsR that contains a PCR amplified  $P_{AA}$ -*arsR* fragment from pAAUN using primers 110709 (5'-AAATCTGAGCTCAATTCCGACGTCTA) and 070817 (5'-CTGCCAGGAATTGGGGATCGGAAG). In this plasmid, *arsR* is under the control of the  $P_{AA}$  promoter and is further downstream of the endogenous  $P_{lac}$  promoter of pGEM-T-Easy.

**Bioreporter Assays. Culture Preparation.** Starting from a single colony, *E. coli* bioreporter strains were grown for 16 h at 37 °C under 160 rpm agitation of the culture flask in LB medium in the presence of 50  $\mu\text{g mL}^{-1}$  kanamycin (Km) to select for the presence of the pAAUN- or pHBP-based reporter plasmids and, when required, 100  $\mu\text{g mL}^{-1}$  ampicillin (Ap) to select for pGEM-pAA-ArsR. The bacterial culture was then 100-fold diluted into fresh LB medium plus Km and incubated for 2 h under 160 rpm agitation until the culture's turbidity at 600 nm had reached between 0.3 and 0.4 (exponentially growing cells). Cells from 10 mL of culture were then harvested by centrifugation at 4000g for 5 min at room temperature. The cell pellet was resuspended into 30 °C preheated MOPS medium to a final optical density at 600 nm of 0.1 (MOPS medium contains 10% [v/v] MOPS buffer, 2 mM  $\text{MgCl}_2$ , 0.1 mM  $\text{CaCl}_2$ , and 2 g of glucose  $\text{L}^{-1}$ , pH 7.0). MOPS buffer itself was prepared with, per liter, 5 g of NaCl, 10 g of  $\text{NH}_4\text{Cl}$ , 98.4 g of 3-([N-morpholino]propanesulfonic acid, sodium salt), 0.59 g of  $\text{Na}_2\text{HPO}_4 \cdot 2\text{H}_2\text{O}$ , and 0.45 g of  $\text{KH}_2\text{PO}_4$ . This cell suspension was subsequently used for the reporter assays.

**Bioreporter Assay Preparation and Readout.** Bioreporter assays were prepared in 96-well microplates (Greiner Bio-One). In the case of a single induction with arsenic, a 180  $\mu\text{L}$  aliquot of the bioreporter cell suspension in MOPS was mixed with 20  $\mu\text{L}$  of an aqueous solution containing between 0 and 1 mg of arsenite ( $\text{AsIII}$ )  $\text{L}^{-1}$ , prepared by serial dilution of a 0.05 M solution of  $\text{NaAsO}_2$  (Merck) in arsenic-free tap water. In the case of induction with 2-hydroxybiphenyl (2HBP), stock solutions were made from 0 to 10 mM 2HBP in pure dimethyl sulfoxide (DMSO), from which working solutions were prepared by dilution of 1:100 in arsenic-free tap water. As a negative control, the same dilution of DMSO in water was added. Reporter assays with double induction were prepared by mixing 160  $\mu\text{L}$  of MOPS bioreporter cell suspension with 20  $\mu\text{L}$  of 2HBP working solution and 20  $\mu\text{L}$  of arsenite aqueous solution. Bioreporter assays were prepared in triplicate and incubated at 30 °C under mixing at 500 rpm for 3 h in the case of single arsenic induction assays and 2 h for the double induction in a 96-well thermostated shaker (THERMOstar, BMG Labtech). After the indicated incubation times, 5  $\mu\text{L}$  of each assay was removed and twice diluted by mixing with 195  $\mu\text{L}$  of distilled water, after which 3  $\mu\text{L}$  was aspired and immediately analyzed on a Becton Dickinson LSR-Fortessa flow cytometer (BD Biosciences, Erembodegem, Belgium).

mCherry fluorescence of individual cells was collected in the Texas-Red channel (610/20 nm), whereas EGFP fluorescence was measured using the FITC channel (530/30 nm).

**Northern Blotting.** Exponentially growing *E. coli* bio-reporter cultures were prepared as before and induced in triplicate with 2HBP (10  $\mu$ M) or 2HBP (10  $\mu$ M) plus arsenite (100  $\mu$ g L<sup>-1</sup>) for 30 min before RNA was isolated. Cell pellets were collected by centrifugation at 20 000g and 4 °C, after which the cells were resuspended and RNA was purified using the hot phenol–chloroform extraction method, as described by Aiba et al.<sup>38</sup> Aliquots of 5  $\mu$ g of total RNA were fractionated on 1% (w/v) agarose gels containing 5% (v/v) formaldehyde and transferred to Hybond-N membrane (Amersham) as described elsewhere.<sup>39</sup> RNA was cross-linked to the membrane using UV irradiation and then prehybridized for 1 h at 42 °C in 5 $\times$  concentrated SSPE buffer containing 1% sodium dodecylsulfate, Denhardt's solution, and 1% blocking reagent (Roche). Oligonucleotide DNA probes were designed and synthesized (Microsynth) to be specific for the Km-resistance gene of pHBP269 (5'-CTTCAGTGACAACGTCGAGCACAGCT), for the *egfp* gene (5'-GAAAATTTGTGCCCATTAACAT-CACCATCT), and for the 5'-UTR immediately downstream of P<sub>C</sub>, common to all pHBP269-based constructs (5'-TTAATAGGCAGCAGTACAGTCGAAGCTC ACGG). All probes had a predicted annealing temperature of 62–63 °C and were labeled at the 5' end with digoxigenin. Hybridization was carried out in 25 mL of buffer with 10 pmol of probe at 60 °C for 1 h, after which the temperature was lowered by 5 °C every 30 min until 40 °C was reached. Probes were further allowed to anneal for 16 h at 40 °C, after which the temperature was lowered by 5 °C every 30 min until room temperature was reached. The membrane was then washed for 15 min with SSPE at room temperature. Probe detection was performed using the DIG luminescent detection kit (Roche) according to the manufacturer's instructions.

**Chemicals.** Unless otherwise mentioned, all chemicals were of the highest available purity and obtained from Sigma-Aldrich.

## ■ ASSOCIATED CONTENT

### ● Supporting Information

The Supporting Information is available free of charge on the ACS Publications website at DOI: 10.1021/acssynbio.5b00111.

Sequence of the ArsR binding site and possible interactions with the ArsR-dimer; sequence detail of plasmid pAA-2ABS+489; reporter output from arsenic responsive circuits with *arsR-mCherry* instead of *arsR* control; cartoon model to explain orientation dependent transcription roadblock effect; cartoon model to explain ArsR-dependent transcription reduction effect from upstream-placed auxiliary operators; sequence detail of pHBP-ABS-dir1 construction (PDF).

## ■ AUTHOR INFORMATION

### Corresponding Author

\*Tel.: +41 21 692 5630. Fax: +41 21 692 5600. E-mail: janroelof.vandermeer@unil.ch.

### Author Contributions

D.M. and J.R.v.d.M. conceived the study. D.M. performed experiments. D.M. and J.R.v.d.M. wrote the article.

### Notes

The authors declare no competing financial interest.

## ■ ACKNOWLEDGMENTS

This work was supported by Swiss National Science Foundation Sinergia (CRSII2-141845) and European Community FP7 ST-FLOW (KBBE-289326) grants. We thank Serge Pelet for critical reviewing of the manuscript.

## ■ ABBREVIATIONS

egfp, enhanced green fluorescence protein; 2HBP, 2-hydroxybiphenyl; UTR, untranslated region; ABS, ArsR binding site (ArsR operator)

## ■ REFERENCES

- (1) Temme, K., Zhao, D., and Voigt, C. A. (2012) Refactoring the nitrogen fixation gene cluster from *Klebsiella oxytoca*. *Proc. Natl. Acad. Sci. U. S. A.* 109, 7085–7090.
- (2) Way, J. C., Collins, J. J., Keasling, J. D., and Silver, P. A. (2014) Integrating biological redesign: where synthetic biology came from and where it needs to go. *Cell* 157, 151–161.
- (3) Alper, H., Fischer, C., Nevoigt, E., and Stephanopoulos, G. (2005) Tuning genetic control through promoter engineering. *Proc. Natl. Acad. Sci. U. S. A.* 102, 12678–12683.
- (4) Chen, Y. J., Liu, P., Nielsen, A. A., Brophy, J. A., Clancy, K., Peterson, T., and Voigt, C. A. (2013) Characterization of 582 natural and synthetic terminators and quantification of their design constraints. *Nat. Methods* 10, 659–664.
- (5) Lou, C., Stanton, B., Chen, Y. J., Munsky, B., and Voigt, C. A. (2012) Ribozyme-based insulator parts buffer synthetic circuits from genetic context. *Nat. Biotechnol.* 30, 1137–1142.
- (6) Moon, T. S., Lou, C., Tamsir, A., Stanton, B. C., and Voigt, C. A. (2012) Genetic programs constructed from layered logic gates in single cells. *Nature* 491, 249–253.
- (7) Stanton, B. C., Nielsen, A. A., Tamsir, A., Clancy, K., Peterson, T., and Voigt, C. A. (2014) Genomic mining of prokaryotic repressors for orthogonal logic gates. *Nat. Chem. Biol.* 10, 99–105.
- (8) Wang, B., Kitney, R. I., Joly, N., and Buck, M. (2011) Engineering modular and orthogonal genetic logic gates for robust digital-like synthetic biology. *Nat. Commun.* 2, 508.
- (9) Eldar, A., and Elowitz, M. B. (2010) Functional roles for noise in genetic circuits. *Nature* 467, 167–173.
- (10) Friedland, A. E., Lu, T. K., Wang, X., Shi, D., Church, G., and Collins, J. J. (2009) Synthetic gene networks that count. *Science* 324, 1199–1202.
- (11) Prindle, A., Samayoa, P., Razinkov, I., Danino, T., Tsimring, L. S., and Hasty, J. (2011) A sensing array of radically coupled genetic 'biopixels'. *Nature* 481, 39–44.
- (12) Stricker, J., Cookson, S., Bennett, M. R., Mather, W. H., Tsimring, L. S., and Hasty, J. (2008) A fast, robust and tunable synthetic gene oscillator. *Nature* 456, 516–519.
- (13) van der Meer, J. R. (2011) *Bacterial Sensors: Synthetic Design and Application Principles*, Morgan & Claypool, San Rafael, CA.
- (14) Hammer, K., Mijakovic, I., and Jensen, P. R. (2006) Synthetic promoter libraries-tuning of gene expression. *Trends Biotechnol.* 24, 53–55.
- (15) Salis, H. M., Mirsky, E. A., and Voigt, C. A. (2009) Automated design of synthetic ribosome binding sites to control protein expression. *Nat. Biotechnol.* 27, 946–950.
- (16) Dvir, S., Velten, L., Sharon, E., Zeevi, D., Carey, L. B., Weinberger, A., and Segal, E. (2013) Deciphering the rules by which 5'-UTR sequences affect protein expression in yeast. *Proc. Natl. Acad. Sci. U. S. A.* 110, E2792–2801.
- (17) Kudla, G., Murray, A. W., Tollervey, D., and Plotkin, J. B. (2009) Coding-sequence determinants of gene expression in *Escherichia coli*. *Science* 324, 255–258.
- (18) van der Meer, J. R., and Belkin, S. (2010) Where microbiology meets microengineering: design and applications of reporter bacteria. *Nat. Rev. Microbiol.* 8, 511–522.

- (19) Lutz, R., and Bujard, H. (1997) Independent and tight regulation of transcriptional units in *Escherichia coli* via the LacR/O, the TetR/O and AraC/I1-I2 regulatory elements. *Nucleic Acids Res.* 25, 1203–1210.
- (20) Tropel, D., and van der Meer, J. R. (2004) Bacterial transcriptional regulators for degradation pathways of aromatic compounds. *Microbiol. Mol. Biol. Rev.* 68, 474–500.
- (21) Balleza, E., Lopez-Bojorquez, L. N., Martinez-Antonio, A., Resendis-Antonio, O., Lozada-Chavez, I., Balderas-Martinez, Y. I., Encarnacion, S., and Collado-Vides, J. (2009) Regulation by transcription factors in bacteria: beyond description. *FEMS Microbiol. Rev.* 33, 133–151.
- (22) Hammar, P., Leroy, P., Mahmutovic, A., Marklund, E. G., Berg, O. G., and Elf, J. (2012) The *lac* repressor displays facilitated diffusion in living cells. *Science* 336, 1595–1598.
- (23) Hao, N., Krishna, S., Ahlgren-Berg, A., Cutts, E. E., Shearwin, K. E., and Dodd, I. B. (2014) Road rules for traffic on DNA-systematic analysis of transcriptional roadblocking in vivo. *Nucleic Acids Res.* 42, 8861–8872.
- (24) Siegfried, K., Endes, C., Bhuiyan, A. F., Kuppardt, A., Mattusch, J., van der Meer, J. R., Chatzinotas, A., and Harms, H. (2012) Field testing of arsenic in groundwater samples of bangladesh using a test kit based on lyophilized bioreporter bacteria. *Environ. Sci. Technol.* 46, 3281–3287.
- (25) Hedges, R. W., and Baumberg, S. (1973) Resistance to arsenic compounds conferred by a plasmid transmissible between strains of *Escherichia coli*. *J. Bacteriol.* 115, 459–460.
- (26) Wu, J., and Rosen, B. P. (1993) Metalloregulated expression of the *ars* operon. *J. Biol. Chem.* 268, 52–58.
- (27) Osman, D., and Cavet, J. S. (2010) Bacterial metal-sensing proteins exemplified by ArsR-SmtB family repressors. *Nat. Prod. Rep.* 27, 668–680.
- (28) Jaspers, M. C., Suske, W. A., Schmid, A., Goslings, D. A., Kohler, H. P., and van der Meer, J. R. (2000) HbpR, a new member of the XylR/DmpR subclass within the NtrC family of bacterial transcriptional activators, regulates expression of 2-hydroxybiphenyl metabolism in *Pseudomonas azelaica* HBP1. *J. Bacteriol.* 182, 405–417.
- (29) Jaspers, M. C., Schmid, A., Sturme, M. H., Goslings, D. A., Kohler, H. P., and van der Meer, J. R. (2001) Transcriptional organization and dynamic expression of the *hbpCAD* genes, which encode the first three enzymes for 2-hydroxybiphenyl degradation in *Pseudomonas azelaica* HBP1. *J. Bacteriol.* 183, 270–279.
- (30) He, B., and Zalkin, H. (1992) Repression of *Escherichia coli purB* is by a transcriptional roadblock mechanism. *J. Bacteriol.* 174, 7121–7127.
- (31) Trang, P. T., Berg, M., Viet, P. H., van Mui, N., and van der Meer, J. R. (2005) Bacterial bioassay for rapid and accurate analysis of arsenic in highly variable groundwater samples. *Environ. Sci. Technol.* 39, 7625–7630.
- (32) Rodriguez-Lado, L., Sun, G., Berg, M., Zhang, Q., Xue, H., Zheng, Q., and Johnson, C. A. (2013) Groundwater arsenic contamination throughout China. *Science* 341, 866–868.
- (33) Fendorf, S., Michael, H. A., and van Geen, A. (2010) Spatial and temporal variations of groundwater arsenic in South and Southeast Asia. *Science* 328, 1123–1127.
- (34) Merulla, D., Hatzimanikatis, V., and van der Meer, J. R. (2013) Tunable reporter signal production in feedback-uncoupled arsenic bioreporters. *Microb. Biotechnol.* 6, 503–514.
- (35) Sambrook, J., and Russell, D. W. (2001) *Molecular Cloning: A Laboratory Manual*, 3rd ed., Cold Spring Harbor Laboratory Press, Cold Spring Harbor, NY.
- (36) Stocker, J., Balluch, D., Gsell, M., Harms, H., Feliciano, J. S., Daunert, S., Malik, K. A., and van der Meer, J. R. (2003) Development of a set of simple bacterial biosensors for quantitative and rapid field measurements of arsenite and arsenate in potable water. *Environ. Sci. Technol.* 37, 4743–4750.
- (37) Beggah, S., Vogne, C., Zenaro, E., and van der Meer, J. R. (2008) Mutant transcription activator isolation via green fluorescent protein based flow cytometry and cell sorting. *Microb. Biotechnol.* 1, 68–78.
- (38) Aiba, H., Adhya, S., and de Crombrughe, B. (1981) Evidence for two functional *gal* promoters in intact *Escherichia coli* cells. *J. Biol. Chem.* 256, 11905–11910.
- (39) Regnier, P., and Hajnsdorf, E. (1991) Decay of mRNA encoding ribosomal protein S15 of *Escherichia coli* is initiated by an RNase E dependent endonucleolytic cleavage that removes the 3' stabilizing stem and loop structure. *J. Mol. Biol.* 217, 283–292.